Journal of Applied Polymer Science

Preparation of grafted cationic polymer/silver chloride modified cellulose fibers and their antibacterial properties

Xiaoqin Chen,[1] Bojian Hu,[2] Xiaodong Xing,[1] Zuliang Liu,[1] Yan Zuo,[1] Qian Xiang[1]

[1]College of Chemical Engineering, Nanjing University of Science and Technology, Nanjing 210094, China

[2]AppTech Company, Limited, Shanghai 200131, China

Correspondence to: X. Xing (E-mail: xingxiaodong07@njust.edu.cn)

ABSTRACT: In this article, we present a simple method for synthesizing antibacterial cellulose fibers that were modified with a cationic polymer and immobilized silver chloride (AgCl) particles. Relatively simple techniques of graft polymerization and onsite precipitation were used to fabricate the composites. Scanning electron microscopy images, Fourier transform infrared spectroscopy, X-ray diffraction, thermogravimetric analysis, and energy-dispersive X-ray spectroscopy confirmed the immobilization of the AgCl particles. The observed inhibition zone of the immobilized AgCl particle composites indicated that the biocidal silver ions were released from the composites in aqueous solution. Compared with cationic-polymer-grafted cellulose fibers or AgCl alone, the cationic polymer/AgCl composites showed excellent antibacterial activity against Gram-negative *Escherichia coli* and Gram-positive *Staphylococcus aureus*. © 2015 Wiley Periodicals, Inc. J. Appl. Polym. Sci. **2015**, *132*, 42092.

KEYWORDS: biomaterials; fibers; grafting

Received 21 November 2014; accepted 10 February 2015

DOI: 10.1002/app.42092

INTRODUCTION

Recently, considerable research effort has been focused on rendering materials with antibacterial properties to prevent infection from pathogenic microorganisms.[1–4] Microbial infestation has been implicated in a variety of detrimental outcomes, including the rejection of medical implants, food spoilage, biofouling of materials, water contamination, and spread of foodborne diseases.[5–9] Because of the potentially daunting complexity of the microbial population and microbial antibiotic resistance, alternative strategies that can completely inhibit bacterial infection are desirable.[10] Hence, the design of antibacterial materials with desirable attributes, such as potent and rapid antibacterial efficacy, is of vital importance. Composite antibacterial materials that act via multiple mechanisms offer a great opportunity to redress this persistent challenge.[11,12] For example, Ho *et al.*[13] reported a network film modified with silver nanoparticles and poly(ethylene glycol), it was capable of killing bacteria and repelling microbes at the same time. Carpenter *et al.*[14] reported dual-action antimicrobial silica nanoparticles modified with immobilized quaternary ammonium salts and releasable nitric oxide.

Silver is recognized as an excellent antibacterial agent for its broad-spectrum bactericidal efficacy, and it does not easily provoke microbial resistance.[15–18] Therefore, silver-containing materials, which consist of either elemental silver or highly water-soluble silver salts, have been used in many cases for disinfection.[19–23] Because the antibacterial abilities of silver-containing materials are attributed to the release of active bactericidal silver ions, many efforts have been made to increase the amount of Ag^+ ions and prolong their release to act as long-acting antibacterial materials.[24] Sparingly soluble silver salts, such as silver halides, significantly increase the rate of generation of biocidal Ag^+ ions over that from elemental silver and limit the uncontrolled dissolution of freely soluble silver species, whereas they provide a controlled dissolution of Ag^+ ion in aqueous environments (AgCl solubility product constant = 1.56×10^{-10}).[25]

Unfortunately, the antibacterial abilities of silver-containing materials would be lost when the contained silver is depleted.[26–28] To improve the antibacterial activity of the materials, much work has been done to composite silver biocide with antibacterial polymers, such as in quaternary ammonium salts [21,29,30] and antimicrobial peptides,[31,32] which are promising for efficient and long-term antimicrobial performance. Through using the advantages of these existing approaches while minimizing their disadvantages, one may achieve these combinations with a highly potent antibacterial efficiency. Quaternary ammonium salts are excellent candidates for their broad-spectrum bactericidal activities and abilities to kill bacteria with no effects on the structure of their own.[13,33] Therefore, they can easily be combined with other bactericides.[16,34,35] For example, Li *et al.*[26] reported two-level antibacterial coatings with a cationic polymer

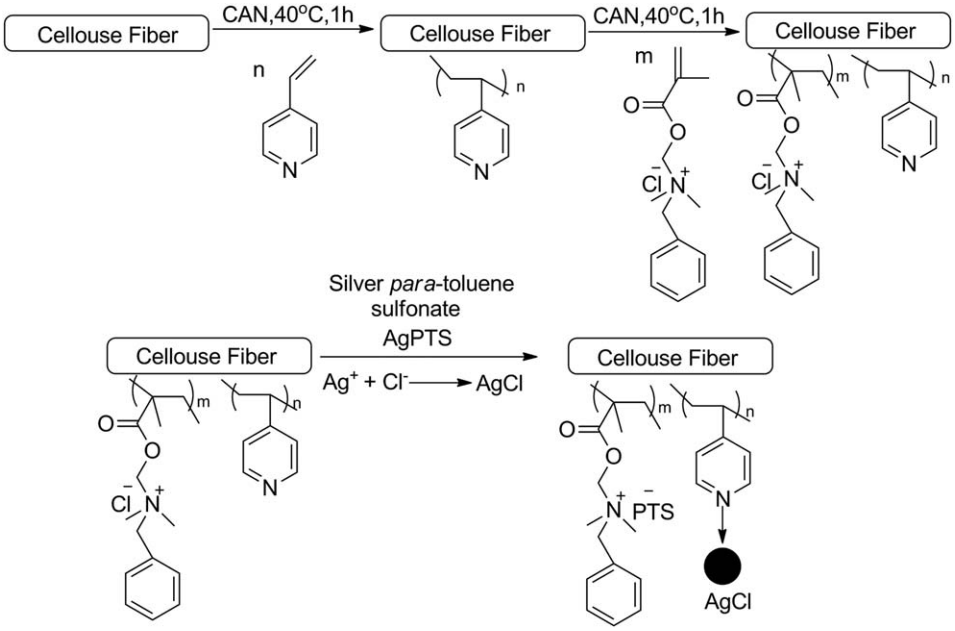

Scheme 1. Schematic of the synthesis procedure for a dual-action antibacterial material(C-*g*-PVPDM/AgCl).

matrix and embedded silver nanoparticles. The composite antibacterial materials provided strong antibacterial activity against both Gram-negative and Gram-positive bacteria.

Cellulose fibers are a good choice for substrates because of their versatility, chemical flexibility, and biodegradability.[36] In this study, antibacterial cellulose fibers were prepared via the grafting of the cationic polymer poly(4-vinylpyridine)-*co*-poly[*N*,*N*-dimethyl-*N*-(methacryloyloxy) ethyl-*N*-benzyl ammonium chloride] onto cellulose. Then, the silver chloride (AgCl) particles were synthesized by the *in situ* precipitation of chloride anions of the quaternary ammonium salts and stabilized by the capping action of the pyridine groups. The antibacterial activities of the composites were evaluated with the modified Kirby–Bauer test and the measurement of antibacterial kinetics. We also showed that by tailoring the concentration of silver ions, we could control the sizes of the immobilized AgCl particles.

EXPERIMENTAL

Materials

The monomer *N*,*N*-dimethyl-*N*-(methacryloyloxy)ethyl-*N*-benzyl ammonium chloride (DMABn) was prepared in our laboratories.[37] Cellulose fiber was purchased from Shanghai DaiDi Medical Equipment Co., Ltd. (China). The 4-vinylpyridine (4-VP) was purchased from Shanghai Aladdin Chemistry Co., Ltd. (China). Silver *para*-toluene sulfonate (AgPTS) was obtained from Tianjin Heowns Biochem LLC (China). The initiator, ceric ammonium nitrate (CAN), was obtained from Adamas Reagent Co., Ltd. (Basel, Switzerland). The other reagents were purchased from Nanjing Chemical Reagent Co., Ltd. (China) and were used without any purification.

Measurements

Scanning electron microscopy (SEM) images with energy-dispersive X-ray spectroscopy (EDS) were obtained on a S-4800 field emission scanning electron microscope at 15.0 kV with a field emission electron gun. The powder X-ray diffraction (XRD) measurements were performed on a Bruker model D8 ADVANCE diffractometer equipped with a copper anode producing X-rays with a wavelength of 1.5418. Fourier transform infrared (FTIR) spectra were carried out with a Shimadzu IR Prestige-21 spectrometer. Thermogravimetric analysis (TGA) were recorded with a Mettler Tory thermogravimetric analyzer.

Preparation of the Cationic-Polymer-Grafted Cellulose Fiber

As shown in Scheme 1, the cationic-polymer-grafted cellulose fibers {cellulose-*graft*-poly(4-vinyl pyridine)-*co*-poly[*N*,*N*-dimethyl-*N*-(methacryloyloxy)ethyl-*N*-benzyl ammonium chloride] (C-*g*-PVPDM)} were fabricated by a two-step graft polymerization. In the first step, cellulose fibers were immersed in 5 mL of deionized water, and an appropriate amount of monomer 4-VP (0.006 mol) was added. Nitrogen was injected for 10 min to exclude air. After the initiator, CAN (0.375 mmol), was added, the reaction was kept at 40°C for 1 h under an N_2 atmosphere. Then, the modified cellulose fibers were washed several times to remove the Ce salt by distilled water, extracted with acetone in a Soxhlet extractor for 12 h to remove the homopolymer and unreacted monomer, and dried before further treatment.

The grafting ratio (W_g) was calculated with the following formula:

$$W_g(\%) = (W_1 - W_0)/W_0 \times 100\% \quad (1)$$

where W_0 is the weight of the dry cellulose fiber before the grafting process and W_1 is the weight of the dry cellulose fiber after grafting with the monomer.

In the second step, the monomer, DMABn (0.0045 mol), was grafted onto the cellulose by repetition of the same reaction process in the first step. Finally, C-*g*-PVPDM was obtained.

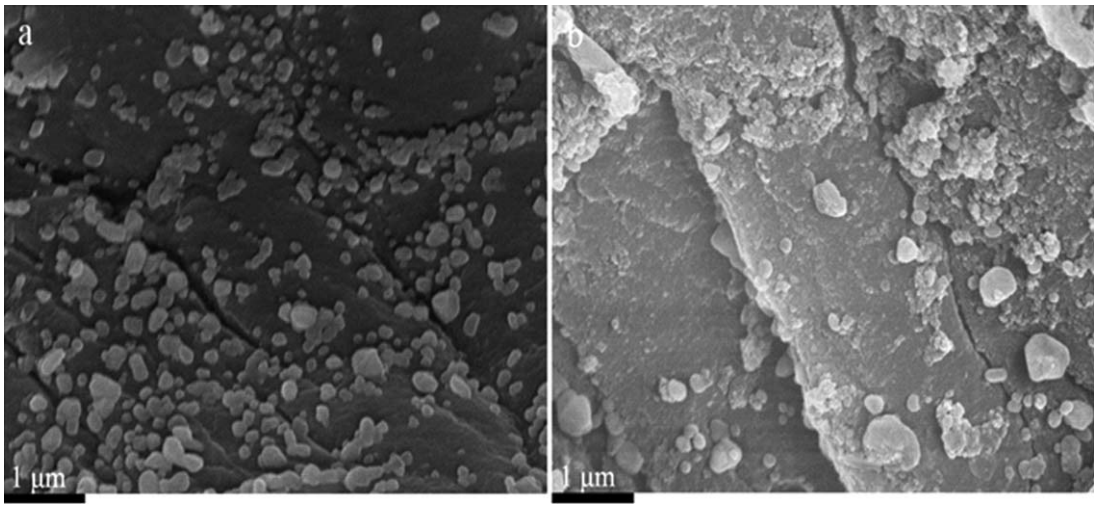

Figure 1. SEM images of (a) C-*g*-PVPDM/AgCl1 and (b) C-*g*-PVPDM/AgCl2.

Precipitation of the AgCl Particles

An appropriate amount of C-*g*-PVPDM and AgPTS were dispersed separately in deionized water and both cooled to 0°C in an ice bath. The AgPTS solution was added dropwise to the C-*g*-PVPDM solution at 0°C, and the mixture was stirred for 1 h at room temperature. The AgCl-containing C-*g*-PVPDM (C-*g*-PVPDM/AgCl) was obtained after the excess chemicals and unstabilized AgCl particles were removed by distilled water.

Antibacterial Testing

Antibacterial tests were conducted by a modified Kirby–Bauer test and kinetic test with *Escherichia coli* and *Staphylococcus aureus* as model bacteria.

For the modified Kirby–Bauer test, the C-*g*-PVPDM/AgCl composites were pressed into disk-shaped filter paper with an approximately diameter of 11 mm. Both the pure cellulose fiber and C-*g*-PVPDM were tested as controls. Separately, 50 μL of a bacterial suspension (10^6-10^7 cfu/mL) was incubated on Luria–Bertani (LB) agar plates, and the sample paper was gently placed on the center. Bacterial growth was visualized after overnight incubation at 37°C, and digital images of the plates were captured. The zone of inhibition was measured to evaluate the antimicrobial efficacy.

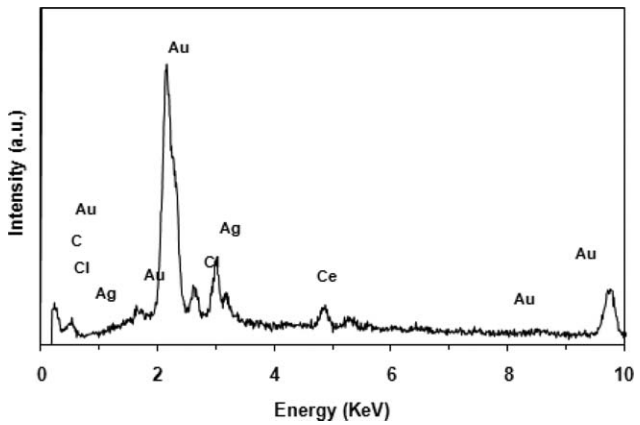

Figure 2. EDS spectrum of C-*g*-PVPDM/AgCl1.

For the kinetic test, *E. coli* and *S. aureus* were incubated in aqueous LB broth overnight at 37°C. The concentration of bacterial suspension used for the tests was 10^6-10^7 cfu/mL. Identical amounts of each species (30 mg) were added to sterile test tubes and inoculated with 3 mL of the bacterial suspension. The initial time of addition of the LB bacteria broth to the tubes was taken as zero, and 100-μL volumes were chosen from each of the test tubes at set time intervals. This solution was further diluted by a factor of 10, and 100 μL of the final solution was cultured in LB agar plates. The plates were kept at 37°C for 24 h, and the number of survival colonies was counted.

RESULTS AND DISCUSSION

Characterization of the Antibacterial Cellulose Fibers

The preparation of C-*g*-PVPDM/AgCl composites by graft polymerization and *in situ* precipitation was schematically depicted in Scheme 1. The grafting ratio of 4-VP in C-*g*-PVPDM was 40%, and the grafting ratio of DMABn in C-*g*-PVPDM was 44%. The chloride anions associated with the polymer side chains of the quaternary ammonium polymer were precipitated

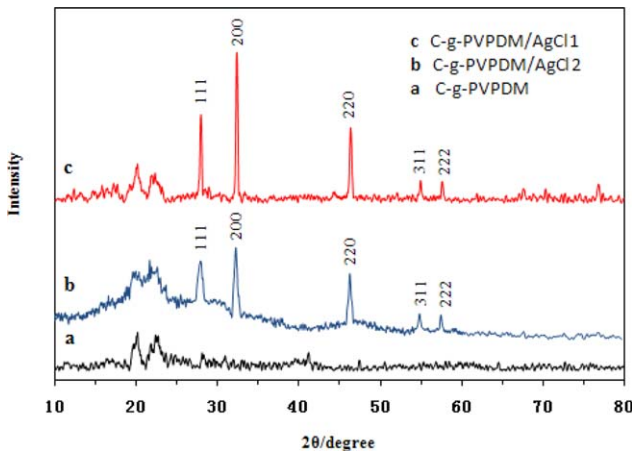

Figure 3. XRD spectra of (a) C-*g*-PVPDM, (b) C-*g*-PVPDM/AgCl2, and (c) C-*g*-PVPDM/AgCl1. [Color figure can be viewed in the online issue, which is available at wileyonlinelibrary.com.]

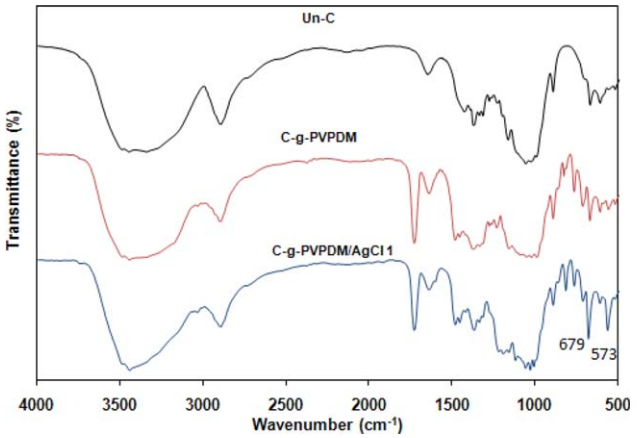

Figure 4. FTIR spectra of Un-C, C-*g*-PVPDM, and C-*g*-PVPDM/AgCl1. [Color figure can be viewed in the online issue, which is available at wileyonlinelibrary.com.]

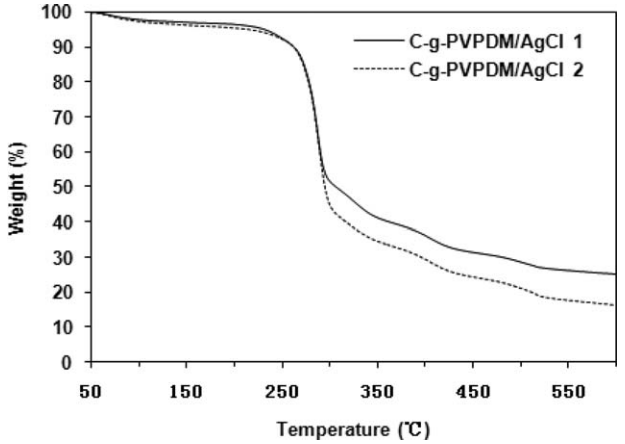

Figure 5. TGA curves of C-*g*-PVPDM/AgCl1 and C-*g*-PVPDM/AgCl2.

by the addition of a silver salt. Via the addition of different amounts of AgPTS, two different AgCl-containing composites, C-*g*-PVPDM/AgCl1 (AgPTS, 0.15 mmol) and C-*g*-PVPDM/AgCl2 (AgPTS, 0.30 mmol) were prepared and studied.

The morphology and sizes of the sample were observed by SEM, as shown in Figure 1. SEM images exhibited the existence of well-defined spherical particles, which were immobilized in the solid polymer of the cellulose fibers. This indicated that monomers were successfully grafted onto the surfaces of the cellulose fiber, and precipitation of AgCl occurred in the vicinity of the polymer chains rather than in solution. The growing AgCl particles were immobilized and prevented from aggregating by the capping action of the pyridine groups. The steric isolation of the grafted polymer chain also helped in the stabilization of particles because the precipitation took place adjacent to them.[21] The concentration of added silver ions had a dramatic impact on the size of the immobilized AgCl particles [Figure 1(a,b)]. A comparison of C-*g*-PVPDM/AgCl1 and C-*g*-PVPDM/AgCl2 showed that the average particle size of C-*g*-PVPDM/AgCl1 (ca. 140 nm) was smaller than that of C-*g*-PVPDM/AgCl2 (ca. 216 nm). As a result, the lower concentration of Ag^+ led to smaller particles. This could be attributed to the higher ratio of capping agent (coordinating pyridine groups) to AgCl in C-*g*-PVPDM/AgCl1 over C-*g*-PVPDM/AgCl2; this resulted in a stronger capping efficiency for the growing particles.

The chemical identity of the observed nanoparticles was further verified by the EDS and powder XRD data, which were collected from the C-*g*-PVPDM/AgCl1 sample. The EDS spectrum demonstrated the existence of Ag and Cl elements (Figure 2), which clearly indicated the presence of AgCl. The Au peaks derived from Au were deposited on the tested sample before measurement.

XRD was used to determine the crystallographic nature of the particles to confirm the immobilized AgCl particles. The XRD patterns of C-*g*-PVPDM, C-*g*-PVPDM/AgCl1, and C-*g*-PVPDM/AgCl2 are shown in Figure 3. Compared with the XRD spectrum of C-*g*-PVPDM, another five major characteristic peaks found at 27.84, 32.26, 46.24, 54.83, and 57.54° corresponded, respectively, to the (111), (200), (220), (311) and (222) crystal planes for C-*g*-PVPDM/AgCl2 and C-*g*-PVPDM/AgCl1; this indicated the presence of a pure cubic phase of AgCl particles.[38] This results show that AgCl was immobilized on the cationic-polymer-grafted cellulose fiber, and the crystalline phase of AgCl was cubic.

To further verify the graft polymerization and immobilization of AgCl, the untreated cellulose fiber (Un-C), C-*g*-PVPDM, and C-*g*-PVPDM/AgCl1 were characterized by FTIR spectroscopy. As shown in Figure 4, the obvious vibrational peak at 1732 cm^{-1} was attributed to the C═O stretching vibrations of the DMABn molecule.[39] After the immobilization of AgCl, two new peaks appeared at 679 and 563 cm^{-1}; these originated from the benzene skeleton vibrations of the *para*-toluene sulfonate counter ion.

The effect of the silver ion concentration on the AgCl amount of C-*g*-PVPDM/AgCl was investigated with TGA. From the TGA information (Figure 5), we concluded that these samples had the same component but different content. The weight loss between 200 and 500°C was attributed to the decomposition of the grafted polymer and cellulose fiber matrix. The residues remaining after pyrolysis were assumed to be a mixture AgCl and cellulose fiber matrix. It was obvious that the amount of residues decreased from 25 to 16 wt % (C-*g*-PVPDM/AgCl1 vs C-*g*-PVPDM/AgCl2) as the increase of added AgPTS. This also might have been due to the higher capping efficiency for C-*g*-PVPDM/AgCl1 derived from the higher capping agent/AgCl ratio.

Antibacterial Effects

The antibacterial performance of the prepared C-*g*-PVPDM/AgCl composites was investigated with a modified Kirby–Bauer technique, as reported previously by Song *et al.*[16] Un-C and C-*g*-PVPDM were also observed as controls. Uniform sized filter papers, which were coated with the same weight of tested samples, were placed on a bed of *E. coli* in an agar plate. The bactericidal activity was measured by the zone of inhibition after incubation at 37°C.

There were clearly zones of inhibition (distinct areas with no bacterial growth) around the C-*g*-PVPDM/AgCl samples [Figure 6(a,b)], At the same time, C-*g*-PVPDM and Un-C showed no signs of inhibition [Figure 6(c,d)]. The observed clear zone of

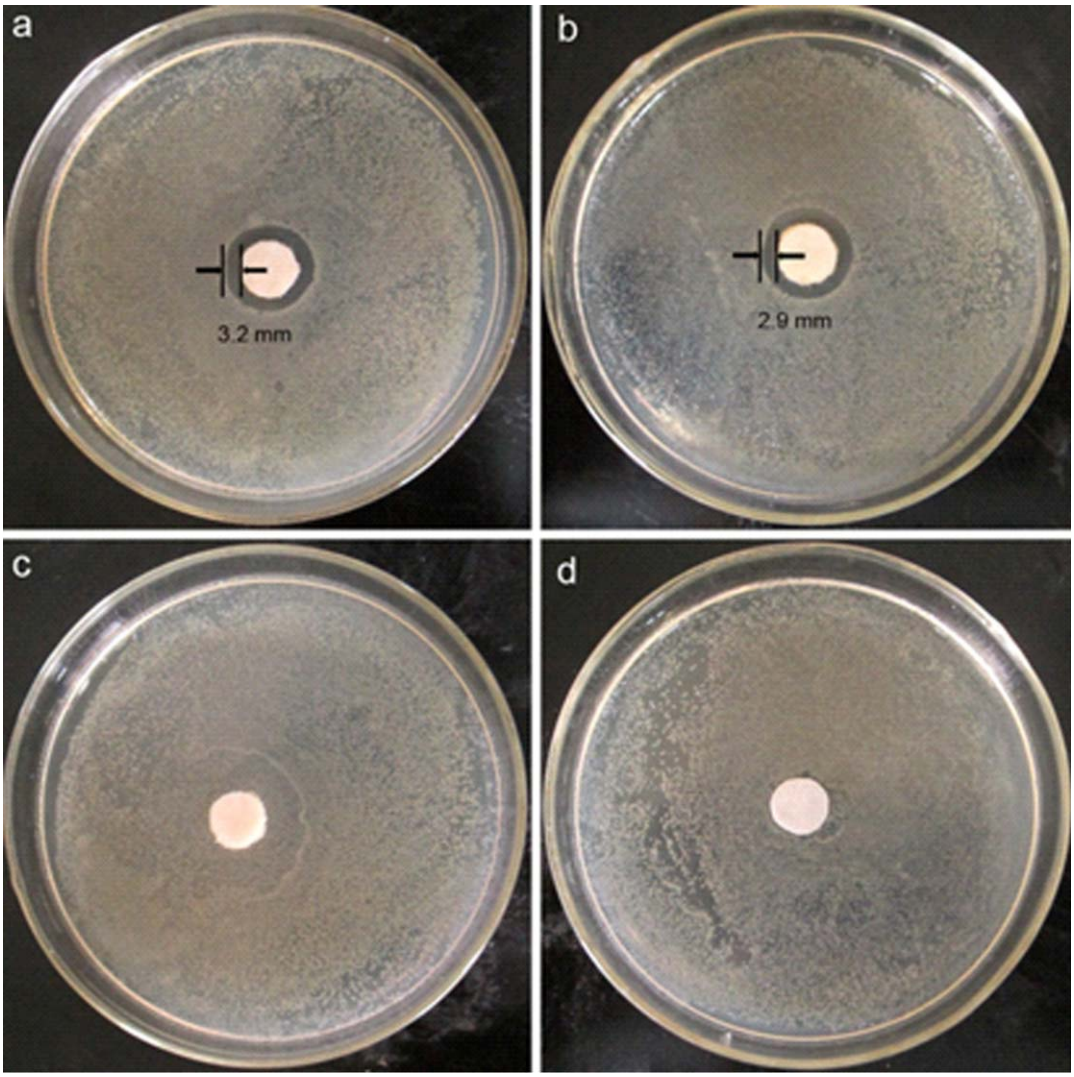

Figure 6. Photographic images of the zones of inhibition of (a) C-*g*-PVPDM/AgCl1, (b) C-*g*-PVPDM/AgCl2, (c) C-*g*-PVPDM, and (d) Un-C against *E. coli*. [Color figure can be viewed in the online issue, which is available at wileyonlinelibrary.com.].

inhibition was a result of the silver ion leaching from C-*g*-PVPDM/AgCl. For C-*g*-PVPDM, the lack of a zone of inhibition could be ascribed to the quaternary ammonium salts were non-depleting antibacterial component. The diameter of the inhibition zone for C-*g*-PVPDM/AgCl1 was 3.2 ± 0.3 mm, and that for C-*g*-PVPDM/AgCl2 was 2.9 ± 0.2 mm [Figure 6(a,b)]. The size of the inhibition zone increased as the AgCl particle size decreased. The smaller AgCl particles had a higher Ag^+ leaching rate; this was probably due to their higher surface-to-volume ratio. Therefore, the leaching rate of silver ions could be controlled by variation of the size of immobilized AgCl particles.

The antimicrobial activity against Gram-negative *E. coli* and Gram-positive *S. aureus* was investigated. The antibacterial properties of C-*g*-PVPDM/AgCl1 and C-*g*-PVPDM/AgCl2 were compared with those of C-*g*-PVPDM and AgCl alone. The C-*g*-PVPDM/AgCl composites possessed enhanced antimicrobial activity compared to the C-*g*-PVPDM for both *E. coli* and *S. aureus* as shown in Figure 7. This could be attributed to the composite antibacterial action mechanism, namely, the bacteria-adsorbing and membrane-disrupting effect of the polymeric quaternary ammonium salts (PQAs)[40] and bactericidal effect of leaching Ag^+.[24] As known, the quaternary ammonium salts quickly adsorbed bacteria while sterilizing them slowly.[37] Therefore, the bacteria adsorbed by PQAs would have priority reaction with the biocidal Ag^+ of C-*g*-PVPDM/AgCl composites. Furthermore, the interaction might become more convenient because the permeability of the cell membrane is altered by PQAs. Thus, through the immobilization of AgCl particles into the grafted cationic polymer layer of cellulose fibers, the C-*g*-PVPDM/AgCl composites showed stronger bactericidal performance. The C-*g*-PVPDM/AgCl1 had a slightly faster suppression rate than the C-*g*-PVPDM/AgCl2; this was presumably a result of the higher loading of AgCl particles and the faster rate of leaching Ag^+ in the former.

CONCLUSIONS

In summary, we prepared a composite antibacterial material modified with cationic polymer and AgCl particles that bore

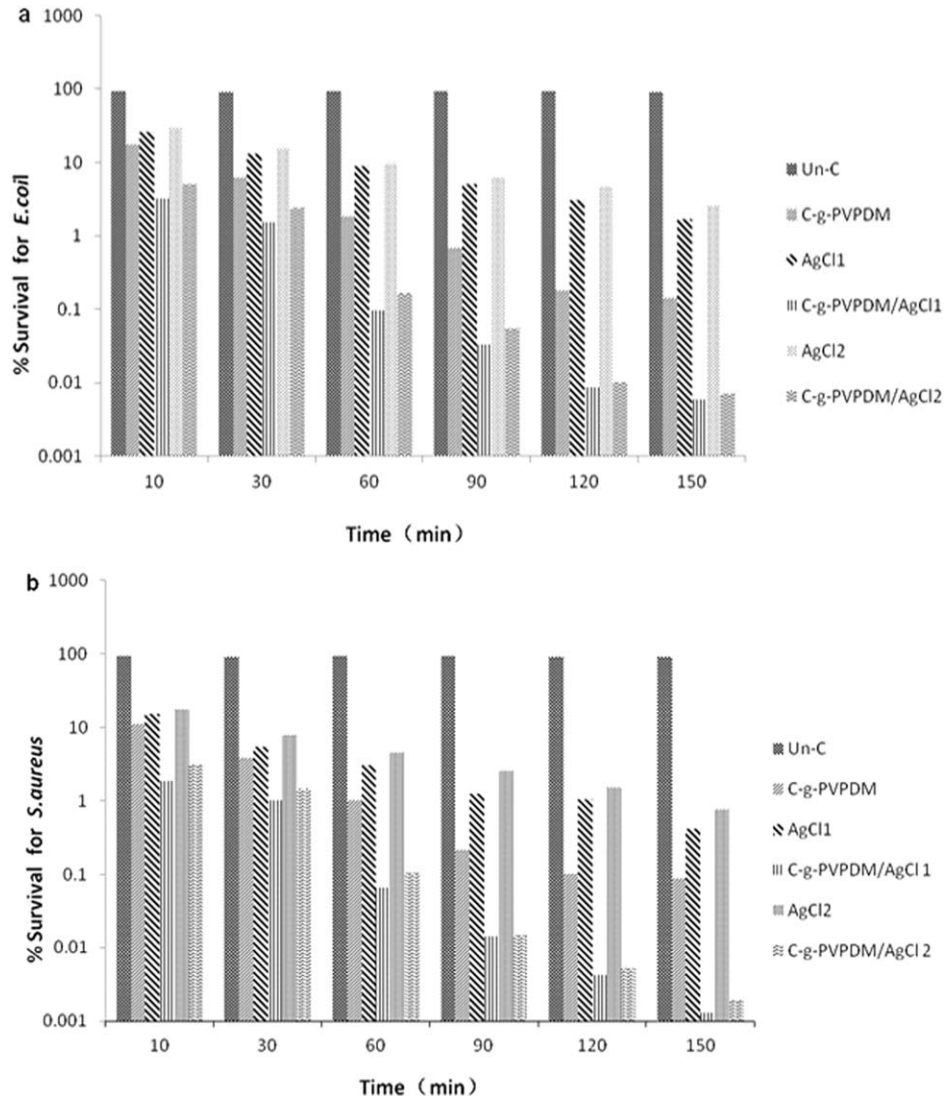

Figure 7. Kinetics of antibacterial activity toward (a) *E. coli* and (b) *S. aureus*: Un-C, C-*g*-PVPDM, AgCl1, C-*g*-PVPDM/AgCl1, AgCl2, and C-*g*-PVPDM/AgCl2.

both a biocide-leaching, bacteria-killing capacity and contact bacteria-killing capacity. The sizes of the immobilized AgCl particles and the leaching rate of Ag^+ could controlled through the variation of the concentration of AgPTS. Compared with C-*g*-PVPDM, the C-*g*-PVPDM/AgCl showed enhanced antibacterial efficiency. According to these results, we anticipate that grafted cationic polymer/AgCl modified cellulose fibers could be applied to a variety of biological applications, such as water sterilization and clinical wound dressings.

ACKNOWLEDGMENTS

This research was supported by the National Natural Science Foundation of China (contract grant number 81130078).

REFERENCES

1. Klibanov, A. M. *J. Mater. Chem.* **2007**, *17*, 2479.
2. Nonaka, T.; Noda, E.; Kurihara, S. *J. Appl. Polym. Sci.* **2000**, *5*, 1077.
3. Suktha, P.; Lekpet, K.; Siwayaprahm, P.; Sawangphruk, M. *J. Appl. Polym. Sci.* **2013**, *6*, 4339.
4. Ferreira, L.; Zumbuehl, A.; Zhu, H. Y.; Yeap, S. H.; Cao, Y.; Qi, X. B.; Zhou, C. C.; Lamrani, M.; Beuerman, R. W.; Kang, E. T.; Mu, Y. G.; Li, C. M.; Chang, M. W.; Leong, S. S. J.; Chan-Park, M. B. *J. Mater. Chem.* **2009**, *19*, 7796.
5. Li, P.; Poon, Y. F.; Li, W.; Zhu, H. Y.; Yeap, S. H.; Cao, Y.; Qi, X. B.; Zhou, C. C.; Lamrani, M.; Beuerman, R. W.; Kang, E. T.; Mu, Y. G.; Li, C. M.; Chang, M. W.; Leong, S. S. J.; Chan-Park, M. B. *Nat. Mater.* **2011**, *10*, 149.
6. Greenberg, C. B.; Steffek, C. *Thin Solid Films* **2005**, *484*, 324.
7. Arciola, C. R.; Campoccia, D.; Gamberini, S.; Donati, M. E.; Pirini, V.; Visai, L.; Speziale, P.; Montanaro, L. *Biomaterials* **2005**, *26*, 6530.
8. Suktha, P.; Lekpet, K.; Siwayaprahm, P.; Sawangphruk, M. *J. Appl. Polym. Sci.* **2013**, *128*, 4339.

9. Martine-Abad, A.; Lagaón, J. M.; Ocio, M. J. *Food Control* **2014**, *43*, 238.
10. Coates, A.; Hu, Y.; Bax, R.; Page, C. *Nat. Rev. Drug Discovery* **2002**, *1*, 895.
11. Jie, Z.; Yan, X.; Zhao, L.; Worley, S. D.; Liang, J. *RSC Adv.* **2014**, *4*, 6048.
12. Hu, B.; Chen, X.; Zuo, Y.; Liu, Z.; Xing, X. *J. Appl. Polym. Sci.* **2014**, *7*, 131.
13. Ho, C. H.; Tobis, J.; Sprich, C.; Thomann, R.; Tiller, J. C. *Adv. Mater.* **2004**, *16*, 957.
14. Carpenter, A. W.; Worley, B. V.; Slomberg, D. L.; Schoenfisch, M. H. *Biomacromolecules* **2012**, *13*, 3334.
15. Kumar, A.; Vemula, P. K.; Ajayan, P. M.; John, G. *Nat. Mater.* **2008**, *7*, 236.
16. Song, J.; Kang, H.; Lee, C.; Hwang, S. H.; Jang, J. *ACS Appl. Mater. Interfaces* **2011**, *4*, 460.
17. Destaye, A. G.; Lin, C. K.; Lee, C. K. *ACS Appl. Mater. Interfaces* **2013**, *5*, 4745.
18. Goli, K. K.; Gera, N.; Liu, X. M.; Rao, B. M.; Rojas, O. J.; Genzer, J. *ACS Appl. Mater. Interfaces* **2013**, *5*, 5298.
19. Nowack, B.; Krug, H. F.; Height, M. *Environ. Sci. Technol.* **2011**, *45*, 7593.
20. Brett, D. W. *Ostomy Wound Manag.* **2006**, *52*, 34.
21. Sambhy, V.; MacBride, M. M.; Peterson, B. R.; Sen, A. *J. Am. Chem. Soc.* **2006**, *128*, 9798.
22. McDonnell, A. M. P.; Beving, D.; Wang, A.; Chen, W.; Yan, Y. *Adv. Funct. Mater.* **2005**, *15*, 336.
23. Vukoje, I. D.; Džunuzović, E. S.; Vodnik, V. V.; Dimitrijević, S.; Ahrenkiel, S. P.; Nedeljković, J. M. *J. Mater. Sci.* **2014**, *49*, 6838.
24. Chernousova, S.; Epple, M. *Angew. Chem. Int. Ed.* **2013**, *52*, 1636.
25. Melaiye, A.; Sun, Z.; Hindi, K.; Milsted, A.; Ely, D.; Reneker, D.; Tessier, C. A.; Youngs, W. J. *J. Am. Chem. Soc.* **2005**, *127*, 2285.
26. Li, Z.; Lee, D.; Sheng, X.; Cohen, R. E.; Rubner, M. F. *Langmuir* **2006**, *22*, 9820.
27. Lichter, J. A.; Van Vliet, K. J.; Rubner, M. F. *Macromolecules* **2009**, *42*, 8573.
28. Podsiadlo, P.; Paternel, S.; Rouillard, J. M.; Zhang, Z.; Lee, J.; Lee, J. W.; Gulari, E.; Kotov, N. A. *Langmuir* **2005**, *12*, 11915.
29. Kong, H.; Jang, J. *Langmuir* **2008**, *24*, 2051.
30. Stevens, K. N.; Knetsch, M. L.; Sen, A.; Sambhy, V.; Koole, L. H. *ACS Appl. Mater. Interfaces* **2009**, *1*, 2049.
31. Ghodake, G.; Lim, S. R.; Lee, D. S. *Colloids Surf. B* **2013**, *108*, 147.
32. Kong, H.; Jang, J. *Biomacromolecules* **2008**, *9*, 2677.
33. Dong, H.; Huang, J.; Koepsel, R. R.; Ye, P.; Russell, A. J.; Matyjaszewski, K. *Biomacromolecules* **2011**, *12*, 1305.
34. Liang, J.; Chen, Y.; Barnes, K.; Wu, R.; Worley, S. D.; Huang, T.-S. *Biomaterials* **2006**, *27*, 2495.
35. Liu, Y. W.; Leng, C.; Chisholm, B.; Stafslien, S.; Majumdar, P.; Chen, Z. *Langmuir* **2013**, *2*, 2897.
36. Frisoni, G.; Baiardo, M.; Scandola, M.; Lednická, D.; Cnockaert, M. C.; Mergaert, J.; Swings, J. *Biomacromolecules* **2001**, *2*, 476.
37. Lu, D. N.; Zhou, X. R.; Xing, X. D.; Wang, X. G.; Liu, Z. *Acta Polym. Sin.* **2004**, *1*, 107.
38. Xu, C.; Yuan, Y.; Cui, A.; Yuan, R. *J. Mater. Sci.* **2013**, *48*, 967.
39. Sun, Y.; Sun, G. *J. Appl. Polym. Sci.* **2001**, *80*, 2460.
40. Alasino, R. V.; Ausar, S. F.; Bianco, I. D.; Castagna, L. F.; Contigiani, M.; Beltramo, D. M. *Macromol. Biosci.* **2005**, *5*, 207.